Letter

Signature of collapsars as sources for high-energy neutrinos and *r*-process nuclei

Gang Guo[1,*] Yong-Zhong Qian[2,†] and Meng-Ru Wu[3,4,‡]

[1]*School of Mathematics and Physics, China University of Geosciences, Wuhan 430074, China*
[2]*School of Physics and Astronomy, University of Minnesota, Minneapolis, Minnesota 55455, USA*
[3]*Institute of Physics, Academia Sinica, Taipei 11529, Taiwan*
[4]*Institute of Astronomy and Astrophysics, Academia Sinica, Taipei 10617, Taiwan*

If collapsars are sources for both high-energy (HE) neutrinos and *r*-process nuclei, then the profuse low-energy antineutrinos from the β decay of the newly synthesized nuclei can annihilate the HE neutrinos. Considering HE neutrinos produced at internal shocks induced by intermittent mildly magnetized jets, we show that such annihilation suppresses the overall HE neutrino spectrum at $\gtrsim 300$ TeV and produces a corresponding flavor composition of $(F_{\nu_e+\bar{\nu}_e}:F_{\nu_\mu+\bar{\nu}_\mu}:F_{\nu_\tau+\bar{\nu}_\tau})_\star \approx (1:10:1)$ at source. We find that the emergent HE neutrino flux can well fit the diffuse flux observed at IceCube if contributions from all similar sources are taken into account. Our results highlight the unique role of HE neutrinos in supporting collapsars as sources for *r*-process nuclei, and can be tested by detection of HE neutrinos from individual sources and accurate measurement of the diffuse HE neutrino flux spectrum and flavor composition.

I. INTRODUCTION

Collapsars produced by the collapse of massive stars into black holes have long been considered a leading candidate for powering type Ibc supernovae and long gamma-ray bursts (GRBs) of both the bright and low-luminosity (LLGRBs) varieties [1–6]. Shocks associated with the propagation of the collapsar jet through the stellar envelope and/or the black-hole accretion disk wind were also proposed as candidate sites for producing $\sim$TeV $-$ PeV high energy (HE) neutrinos [7–27]. These neutrinos may contribute significantly to the diffuse flux detected by IceCube, whose astrophysical origin remains unknown despite recent reports of potential association of several events with a blazar [28,29], three tidal disruption events [30–32], and an active galaxy [33].

The groundbreaking multimessenger observations of GW170817 linked binary neutron star mergers (BNSMs) to both short GRBs and the production of heavy elements beyond iron via the rapid neutron-capture process (*r* process) [34–42]. The astrophysical environments of BNSMs and collapsars are rather similar in that both host accretion disks and the associated jets, thereby producing GRBs and potentially HE neutrinos. Interestingly, Ref. [43] showed that the physical conditions of disk outflows in collapsars resemble those of outflows in BNSMs and

proposed that collapsars are a likely or even the dominant site for producing *r*-process nuclei. This proposal remains hotly debated and requires further theoretical and observational efforts to clarify [44–54].

In this work, we investigate for the first time a novel connection between HE neutrinos and *r*-process nucleosynthesis in collapsars. Unstable neutron-rich heavy nuclei are produced by rapid neutron capture during the *r* process. Their β decay produces $\bar{\nu}_e$ with energy $E_L \sim 4$ MeV on a timescale of ~ 1 s everywhere inside the outflow that expands with a typical velocity $v_{ej} \sim (0.05$–$0.3)c$ (see Fig. 1). Following flavor oscillations, these low energy (LE) antineutrinos can annihilate HE neutrinos of the corresponding flavor produced by shocks at radius R. Efficient annihilation via the Z resonance requires $s = 2E_H E_L(1 - \cos\theta) \sim m_Z^2$, where $\theta \sim \mathcal{O}(1)$ is the intersection angle and m_Z is the Z mass. Therefore, the HE neutrino flux at $E_H \gtrsim \mathcal{O}(100$–$1000)$ TeV is expected to be affected. As we will show, such annihilation can leave clear imprints on the energy spectrum and flavor composition of the emergent HE neutrinos.

II. ANTINEUTRINOS FROM β DECAY

The β decay of the newly synthesized *r*-process nuclei not only produces a profuse $\bar{\nu}_e$ flux, but also provides a dominant source of energy to heat the associated ejecta [55]. We estimate the $\bar{\nu}_e$ emission using the power generated by β decay. In our benchmark study, we simply assume that the ejecta expands with a constant velocity v_{ej}, forming a

*guogang@cug.edu.cn
†qian@physics.umn.edu
‡mwu@gate.sinica.edu.tw

steady spherical "wind" with a constant mass outflow rate $\dot{M}$ (see the Supplemental Material [56] for discussion of asymmetric winds). As the ejecta expands, the power generated by β decay per unit mass stays almost constant for a period of $\sim T_r$ when the r process produces neutron-rich nuclei far from stability. After neutron capture ceases, that power approximately follows a power-law decline. We take $\dot{\epsilon}_{\bar{\nu}_e,0}\eta(t)$ as the part of the power per unit mass that is carried away by $\bar{\nu}_e$, where $\dot{\epsilon}_{\bar{\nu}_e,0}$ sets the magnitude and $\eta(t)$ characterizes the time evolution with $\eta(0) \approx 1$. From numerical calculations, $\eta(t)$ can be fitted as [57]

$$\eta(t) \approx \left[\frac{1}{2} - \frac{1}{\pi}\arctan\left(\frac{t - T_r}{0.11\ \mathrm{s}}\right)\right]^{1.3}. \quad (1)$$

Ignoring nuclear shell effects and Coulomb correction, we simply take the $\bar{\nu}_e$ spectrum to be $\propto E^2(Q - E)^2$ with Q being the Q value. The energy-differential emission rate of $\bar{\nu}_e$ per unit mass (i.e., emissivity) at radius $r = v_{\mathrm{ej}}t$ can be estimated as

$$j_{\bar{\nu}_e}(E, r) = \frac{\dot{\epsilon}_{\bar{\nu}_e,0}\eta(r/v_{\mathrm{ej}})}{\langle E_L \rangle}\left[\frac{15(2\langle E_L \rangle - E)^2 E^2}{16\langle E_L \rangle^5}\right], \quad (2)$$

where the term in the brackets is the approximate normalized $\bar{\nu}_e$ spectrum with an average energy of $\langle E_L \rangle = Q/2 = 4$ MeV. Note that both $\dot{\epsilon}_{\bar{\nu}_e,0}$ and T_r depend on the electron fraction Y_e of the ejecta [57]. Assuming a typical value of $Y_e = 0.2$ for collapsar outflows and guided by the power used in Ref. [58], we take $\dot{\epsilon}_{\bar{\nu}_e,0} = 5 \times 10^{18}$ erg/g/s and $T_r = 0.4$ s.

The $\bar{\nu}_e$ emission is approximately isotropic. Referring to Fig. 1, we estimate the $\bar{\nu}_e$ intensity (in units of cm^{-2} s^{-1} MeV^{-1} sr^{-1}) at radius R and angle θ by integrating the emissivity along the path length l:

$$I_{\bar{\nu}_e}(E, R, \theta) = \int \frac{\rho(r)j_{\bar{\nu}_e}(E, r)}{4\pi}dl,$$
$$= \frac{R\dot{M}}{16\pi^2 v_{\mathrm{ej}}}\int \frac{j_{\bar{\nu}_e}(E, r)\sin\theta}{r^2\sin^2(\theta + \theta')}d\theta', \quad (3)$$

where $\rho(r) = \dot{M}/(4\pi r^2 v_{\mathrm{ej}})$ is the mass density of the ejecta at radius r, and r is a function of R, θ, and θ'. Unless noted otherwise, we take $\dot{M} = 0.02 M_\odot/$s [53,59] and $v_{\mathrm{ej}} = 0.05c$ [2,47]. The corresponding total number density of LE $\bar{\nu}_e$ at $R \sim 10^{10}$ cm is $\sim 10^{23}$ cm^{-3}.

Following production, the LE $\bar{\nu}_e$ undergo flavor oscillations prior to interacting with the HE neutrinos. The oscillation scenario depends on the matter densities at the $\bar{\nu}_e$ emission site and the interaction site. We consider three sets of probabilities $P_{\bar{\nu}_\alpha}$ for the initial $\bar{\nu}_e$ to be a $\bar{\nu}_\alpha$ at the interaction site: $(P_{\bar{\nu}_e}, P_{\bar{\nu}_\mu}, P_{\bar{\nu}_\tau}) \approx (0.55, 0.18, 0.27)$ (pure vacuum oscillations), $(0.675, 0.095, 0.23)$ (NH), and $(0.022, 0.545, 0.433)$ (IH). The latter two sets assume adiabatic flavor evolution following emission at high densities for
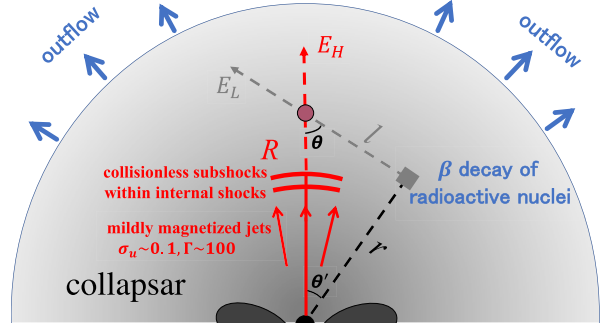

FIG. 1. Sketch of production of HE neutrinos (with energy E_H) and their annihilation with LE antineutrinos (with energy E_L) from β decay of r-process nuclei in a collapsar.

normal (NH) and inverted (IH) neutrino mass hierarchy, respectively (see the Supplemental Material [56]).

III. HIGH-ENERGY NEUTRINO PRODUCTION

Relativistic jets in collapsars induce shocks that can accelerate electrons and protons. The accelerated electrons can produce γ rays or x rays through synchrotron radiation or inverse Compton scattering, thereby making bright GRBs, while the HE protons can collide with photons or stellar matter to make $\pi^\pm$ and $K^\pm$, thereby producing HE neutrinos through meson decays. Shocks emerging at different sites during jet propagation lead to different scenarios for HE neutrino production [60–74]. To demonstrate the effects of LE antineutrinos from β decay, we focus on HE neutrinos produced during jet propagation deep inside the progenitors of collapsars. Specifically, we consider proton acceleration at internal shocks before jet collimation [7,15].

Reference [15] emphasized that shocks inside stars are likely mediated by radiation and in contrast to collisionless shocks [75,76], may not support efficient particle acceleration and HE neutrino production. It was shown later, however, that if the jets are mildly magnetized, then a strong collisionless subshock may occur within the radiation-mediated shock [77,78] to allow particle acceleration at, e.g., mildly relativistic internal shocks [79]. Indeed, using relativistic magnetohydrodynamic simulations of magnetized jets from BNSMs, Ref. [80] found that subshocks can emerge at small radii and produce HE neutrinos at internal shocks, collimation shocks, and shock breakout.

Interestingly, a mild magnetization is also essential to avoid heavy baryon loading of the jets from mixing with the cocoon material [80–82]. With negligible jet-cocoon mixing, the jet Lorentz factor could grow almost linearly with radius due to adiabatic expansion (see, e.g., [83–85]) and reach $\gtrsim 100$ deep inside the star [82,86]. Internal shocks caused by collisions of slow and rapid jets can occur at $R_{\mathrm{is}} \approx \Gamma_s^2 c\delta t = 3 \times 10^9 \Gamma_{s,1}^2 \delta t_{-3}$ cm, where Γ_s is the typical Lorentz factor of the slow jets and δt is the variability timescale. Here and below, $A_x = A/10^x$, where A, if dimensional, is in cgs units. We assume that the typical Lorentz

TABLE I.   Proper values of magnetic field $B_{d(u)}$, proton number density $n_{p,d(u)}$, and photon temperature $T_{\gamma,d(u)}$ in the shocked (downstream) and unshocked (upstream) jets.

	$B_{d(u),8}$	$n_{p,d(u),19}$	$T_{\gamma,d(u),\mathrm{keV}}$
Downstream	$8.2(\epsilon_{B,d}L_{\mathrm{iso},52})^{1/2}/(R_{\mathrm{is},10}\Gamma_2)$	$1.8L_{\mathrm{iso},52}(1-\epsilon_{e,d}-\epsilon_{B,d})R_{\mathrm{is},10}^{-2}\Gamma_2^{-2}$	$3.7(\epsilon_{e,d}L_{\mathrm{iso},52})^{1/4}R_{\mathrm{is},10}^{-1/2}\Gamma_2^{-1/2}$
Upstream	$B_{d,8}/\xi$	$n_{p,d,19}/\xi$	$T_{\gamma,d,\mathrm{keV}}(\epsilon_{e,u}/\epsilon_{e,d})^{1/4}(\Gamma/\Gamma_r)^{1/2}$

factor Γ_r of the unshocked rapid jets is twice the Lorentz factor Γ of the shocked jet. The relative Lorentz factor between the two is $\Gamma_{\mathrm{rel}} \approx \Gamma_r/(2\Gamma) + \Gamma/(2\Gamma_r) = 1.25$, consistent with the mildly relativistic shock.

In our scenario, a strong collisionless subshock forms within the internal radiation-mediated shock to facilitate particle acceleration. This scenario requires $\sigma_u \equiv B_u^2/(4\pi\rho_u c^2) \gtrsim 0.01$ [77,78], where B_u and ρ_u are the proper magnetic field and mass density, respectively, of the unshocked upstream region. Due to shock compression, the magnetic field is amplified to $B_d = \xi B_u$ in the shocked downstream region with the compression ratio $\xi \sim 5$ for $\Gamma_{\mathrm{rel}} \approx 1.25$ [77]. Because HE neutrino flux would be strongly suppressed by synchrotron cooling of $\pi^\pm$ and $K^\pm$ in the enhanced magnetic field B_d, we focus on HE neutrino production via pp and $p\gamma$ reactions in the upstream region (i.e., the unshocked jet), which was barely discussed in previous literature. For radiation-dominated jets at launching, the initial jet temperature is $\sim 1.3L_{\mathrm{iso},52}^{1/4}$ MeV at $r = 10^7$ cm [6]. The jets expand adiabatically and the temperature decreases as r^{-1}. At $r = 10^9$–10^{10} cm, the jet temperature remains a few keV, corresponding to a thermal energy fraction $\epsilon_{e,u} \gtrsim 0.1$. Proper values of magnetic field, proton number density, and photon temperature in the shocked and unshocked jets are given in Table I.

Protons can be accelerated to high energies by crossing the shock fronts repeatedly. During this process, protons have significant probabilities to escape from both the upstream and downstream regions, resulting in a power-law spectrum [87]. Recent simulations of mildly relativistic shocks showed that the accelerated protons in the upstream region are much more abundant than those in the downstream region (see Figs. 7 and 8 of [79]). To obtain a conservative estimate of the maximal proton energy $E_{p,\mathrm{max}}$, we compare the timescales of shock acceleration and different cooling processes for protons in the shocked jet (see the Supplemental Material [56]). For all the parameter sets adopted in this work, the $E_{p,\mathrm{max}}$ computed in the rest frame of the shocked jet is always sufficient to make PeV neutrinos ($E_\nu \sim 0.05\Gamma E_p$ from pp and $p\gamma$ reactions).

We take the (unnormalized) spectrum of the accelerated protons to be $\phi_p(E_p) = E_p^{-2}\exp(-E_p/E_{p,\mathrm{max}})$, and use PYTHIA 8.3 [88] and SOPHIA [89] for pp and $p\gamma$ reactions, respectively, to obtain the $\pi^\pm$ and $K^\pm$ yields at different center-of-mass energies. Because the shocked jet is only mildly relativistic relative to the rapid jet ($\Gamma_{\mathrm{rel}} = 1.25$), we ignore the Lorentz transformation for E_p and $\phi_p(E_p)$ in our

calculations. We include cooling of $\pi^\pm$ and $K^\pm$ due to synchrotron radiation, inverse Compton scattering, $e^\pm$ pair production on photons ($\pi^\pm/K^\pm + \gamma \rightarrow \pi^\pm/K^\pm + e^+ + e^-$), hadronic scattering, and adiabatic expansion (see the Supplemental Material [56]).

In our benchmark study, we take $R_{\mathrm{is}} = 3 \times 10^9$ cm, $L_{\mathrm{iso}} = 10^{53}$ erg/s, $\Gamma_r = 2\Gamma \approx 90L_{\mathrm{iso},49}^{0.18} \approx 472$ [90], $\sigma_d = \xi\sigma_u \approx 2\epsilon_{B,d} = 0.25$, $\xi = 5$, $\epsilon_{e,d} = 0.5$, and $\epsilon_{e,u} = 0.3$ (see Table I). The corresponding $E_{p,\mathrm{max}}$ is $\approx 10^6$ GeV, and we take $E_{p,\mathrm{min}} = 100$ GeV without affecting the results. We find that $e^\pm$ production on photons and synchrotron radiation dominate the cooling of $\pi^\pm$ and $K^\pm$ (see the Supplemental Material [56]). The benchmark HE neutrino spectra are shown in Fig. 2. The competition between pp and $p\gamma$ reactions depends on the effective threshold for meson production and the number density of targets. The pp reaction dominates at low proton energies and produces almost equal neutrino and antineutrino fluxes at $E \lesssim 30$ TeV (left panel) due to equal production of $\pi^+(K^+)$ and $\pi^-(K^-)$. Once the proton energy exceeds the effective threshold for the $p\gamma$ reaction, this reaction dominates due to the much larger number density of thermal photons and gives rise to higher fluxes of neutrinos than antineutrinos (left panel) due to dominant production of $\pi^+(K^+)$ over $\pi^-(K^-)$ and stronger synchrotron cooling of $\mu^\pm$. The latter effect also suppresses production of ν_e and $\bar{\nu}_e$ from $\mu^\pm$ decay compared to that of ν_μ and $\bar{\nu}_\mu$ from $\pi^\pm(K^\pm)$ decay (middle panel).

To cover a wide range of GRB luminosities, we compare the all-flavor neutrino spectra in the right panel of Fig. 2 using $L_{\mathrm{iso}} = 10^{50}$–$10^{53}$ erg/s with other parameters unchanged. The variations with increasing L_{iso} are caused by the boost of neutrino energy due to a larger Lorentz factor and by more efficient cooling of charged mesons at relatively low energies due to a larger photon density or B_u. For $L_{\mathrm{iso}} = 10^{53}$ erg/s, cooling by pair production and synchrotron radiation suppresses neutrino production from $\pi^\pm$ decay so much that $K^\pm$ decay produces half of the neutrinos at 100 TeV.

IV. ANNIHILATION OF HIGH-ENERGY NEUTRINOS WITH LOW-ENERGY ANTINEUTRINOS

Simulations show that the nonrelativistic radioactive outflows occur within a few seconds of jet launching and last for a time comparable to the jet duration [52,53].
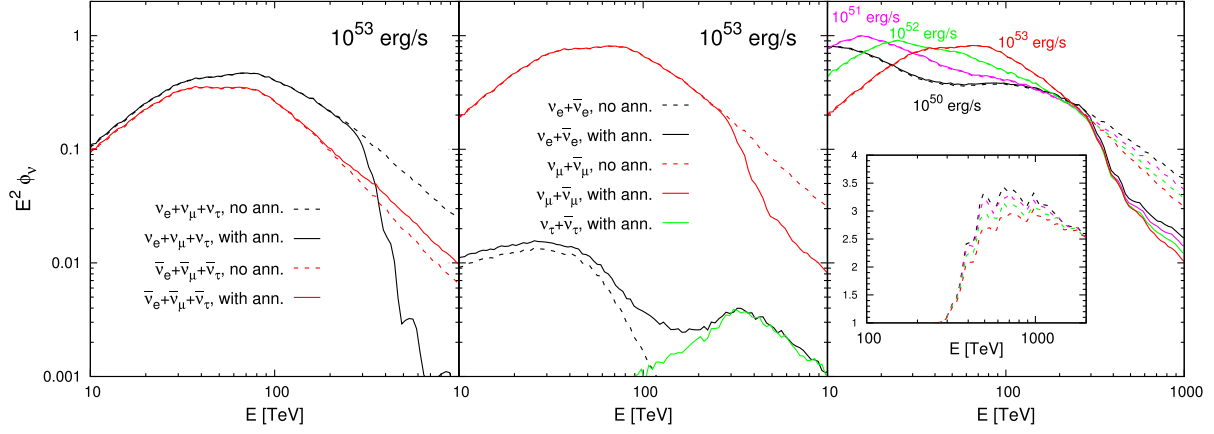
FIG. 2. HE neutrino spectra including annihilation with LE antineutrinos (solid curves) or not (dashed curves). Vacuum oscillations of LE antineutrinos are assumed. The benchmark case with $L_{\rm iso} = 10^{53}$ erg/s is shown in the left ($\nu_e + \nu_\mu + \nu_\tau$ and $\bar{\nu}_e + \bar{\nu}_\mu + \bar{\nu}_\tau$) and middle ($\nu_\alpha + \bar{\nu}_\alpha$ with $\alpha = e, \mu, \tau$) panels. Cases of $L_{\rm iso} = 10^{50}$–10^{53} erg/s are shown in the right panel (all flavors). The inset shows the ratios of all-flavor spectra without annihilation to those with annihilation.

Therefore, most of the HE neutrinos produced at $R_{\rm is} \sim 10^9$–10^{10} cm can meet the LE antineutrinos from the radioactive outflows. The resulting annihilation takes $\lesssim 1$ s, which is significantly shorter than the outflow duration. We use a one-dimensional Monte Carlo code to simulate the propagation of HE neutrinos in the LE antineutrino background and the accompanying processes, which include $\nu_\alpha \bar{\nu}_\alpha$ annihilation and decays of the produced $\pi^\pm$ and $K^\pm$. Note that we also include the annihilation of the regenerated HE ν_α from the earlier annihilation processes. The radial step ΔR to the next interaction point for an HE ν_α with energy E_H at radius R is determined by $\tau_\alpha(E_H, R, \Delta R) = -\ln \lambda$, where τ_α is the optical depth due to $\nu_\alpha \bar{\nu}_\alpha$ annihilation and λ is a random number between 0 and 1. The relevant cross section $\sigma_{\nu_\alpha \bar{\nu}_\alpha}(s)$ peaks at $s = m_Z^2$, and we use PYTHIA 8.3 [88] to track the final products for all s values.

Assuming vacuum oscillations of LE antineutrinos prior to annihilation, we show the spectra of HE neutrinos following annihilation in Fig. 2. The Z resonance starts to occur at $E \sim 300$ TeV. Beyond this energy, the HE neutrino flux drops but the HE antineutrino flux slightly increases due to production from Z decay (left panel). HE neutrinos at these energies are mostly ν_μ, which are annihilated by the LE $\bar{\nu}_\mu$ (middle panel). Strikingly, the ν_e and $\bar{\nu}_e$ regenerated from such annihilation are even more abundant than those produced without annihilation. Consequently, the flux of $\nu_e + \bar{\nu}_e$ is very similar to that of the regenerated $\nu_\tau + \bar{\nu}_\tau$ at $E \gtrsim 300$ TeV following annihilation (middle panel). The above effects produce a unique flavor composition of $(F_{\nu_e + \bar{\nu}_e} : F_{\nu_\mu + \bar{\nu}_\mu} : F_{\nu_\tau + \bar{\nu}_\tau})_\star \approx (1 : 10 : 1)$ for $E \gtrsim 300$ TeV at source, which corresponds to a normalized composition of $\approx (0.21 : 0.42 : 0.37)$ at Earth following vacuum oscillations. The corresponding all-flavor spectrum with the suppression due to annihilation is shown in the right panel of Fig. 2 for different values of

$L_{\rm iso}$. With an optical depth of 3–8 for $\nu_\mu \bar{\nu}_\mu$ annihilation for $E_H \sim 0.4$–1 PeV, the suppression factor can be as high as 3–3.5 (see the inset in the right panel of Fig. 2).

V. DIFFUSE NEUTRINO FLUX

Although prompt HE neutrinos associated with bright GRBs are tightly constrained by IceCube [91–95], subleading contributions of precursor neutrinos from jet propagation inside stellar matter still remain possible. The most recent analyses showed that precursor neutrinos preceding the prompt γ rays by tens of seconds are limited to $\lesssim 10\%$ of the diffuse flux at $E = 100$ TeV (see Fig. 7 of [95]). On the other hand, LLGRBs, whose rate is ~ 10 times higher than that of classical GRBs [96–98], could be caused by a shock breakout driven by a relativistic jet propagating into an extended envelope [4]. They may have a common collapsar origin and host jets with similar luminosities inside stars to those for bright GRBs [21,98]. Note that, in the shock breakout scenario, the observed γ-ray luminosities of LLGRBs ($L_{\gamma,{\rm llgrb}}^{\rm obs} \sim 10^{46}$–$10^{48}$ erg/s) are much lower than those of bright GRBs because the emission for LLGRBs spans a longer duration ($\Delta T_{\gamma,{\rm llgrb}} \sim 10^3$–$10^4$ s) as determined by the large shock breakout radius and is over a wider opening angle ($\theta_{\rm llgrb} \sim 1$ rad). Considering the duration correction, the beam factor correction, and a baryon loading factor $f_p \sim 10$, the true luminosity of LLGRB jets initially launched inside stars could be $L_{\rm iso} \sim L_{\gamma,{\rm llgrb}}^{\rm obs} f_p \frac{\Delta T_{\gamma,{\rm llgrb}}}{\Delta T_{\rm eng}} \frac{\theta_{\rm llgrb}^2}{\theta_j^2} \sim 10^{51}$–$10^{53}$ erg/s, where $\Delta T_{\rm eng} \sim 10$–100 s is the central engine duration and $\theta_j \sim 0.1$ rad is the initial jet opening angle at launch. As HE neutrinos are produced deep inside stars in our work, LLGRBs and bright GRBs are similar sources for HE neutrinos, except that they have different occurrence rates. Further, choked collapsar jets could be even more common than bright GRBs and LLGRBs if the central engine is not active for too

long [99]. To incorporate contributions from all similar sources, we introduce the parameter $f_\star$ as the ratio of the total rate of collapsars with mildly magnetized jets to that of bright GRBs.

The unnormalized HE neutrino spectrum from a single source is shown in Fig. 2. To obtain the diffuse neutrino flux from all similar sources over cosmic history, we multiply the unnormalized spectrum by the following factor [15]

$$\frac{c}{4\pi H_0} \frac{f_z f_\star \dot{n}_{\text{GRB}} f_{\text{cr}} E_{\text{iso}}}{\ln(E_{p,\text{max}}/E_{p,\text{min}})} \frac{1}{\text{GeV cm}^{-2} \text{ s}^{-1} \text{ sr}^{-1}}$$

$$\sim 7 \times 10^{-9} \left(\frac{f_z f_\star \dot{n}_{\text{GRB}}}{\text{Gpc}^{-3} \text{ yr}^{-1}} \right) f_{\text{cr}} E_{\text{iso},53}, \qquad (4)$$

where $f_z \sim 3$ accounts for evolution of source population and neutrino energy with redshift z [100], $\dot{n}_{\text{GRB}} \sim 1$ Gpc^{-3} yr^{-1} is the rate of bright GRBs per unit volume, E_{iso} is the total isotropic energy of jets, and f_{cr} is the fraction of jet energy converted into HE protons. Taking $f_\star = 10$, $f_{\text{cr}} E_{\text{iso},53} \sim 1$, and assuming that contributions from sources at $z \sim 1$ dominate, we compare the all-flavor $E^2 F_\nu(E)$ from our model to the IceCube data [101] in Fig. 3. It can be seen that LLGRBs and choked jets with collapsar origin may explain the observed TeV–PeV flux at IceCube. More interestingly, the spectrum with suppression at $E \gtrsim 100$–200 TeV due to annihilation (and redshift) leads to better agreement with data than that without annihilation. Results using $\dot{M} = 0.01$ and $0.05 M_\odot/\text{s}$ are also shown for comparison. Note that spherical winds and vacuum oscillations of LE antineutrinos are assumed for our benchmark study. The annihilation effect could be similar or even enhanced for asymmetric winds while it will be reduced for the NH oscillation scenario with a
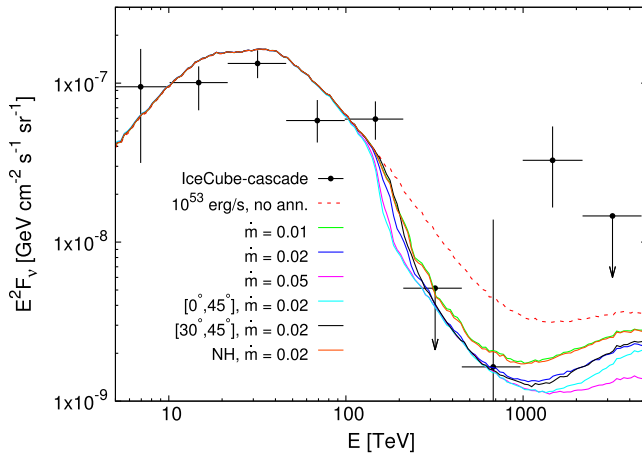

FIG. 3. All-flavor diffuse neutrino flux spectra from our collapsar model with and without annihilation compared to IceCube data [101]. Contributions from jets with $L_{\text{iso},53} = 1$ at redshift $z = 1$ are assumed to dominate. Results for different values of $\dot{m} \equiv \dot{M}/(M_\odot/\text{s})$, asymmetric winds confined to $\theta' = [0°, 45°]$ and $[30°, 45°]$, and the NH oscillation scenario for LE antineutrinos are also shown.

smaller $P_{\bar{\nu}_\mu}$ (see the Supplemental Material [56]). We find that annihilation is significant under a range of assumptions (see Fig. 3). Our model, however, cannot account for the PeV events detected at IceCube despite the production of a small bump above ~ 1 PeV associated with a minimum in the timescale for cooling of $K^\pm$ by pair production (see Fig. 3 of the Supplemental Material [56]). Another source is required for these events [24,102–105].

VI. SUMMARY AND DISCUSSION

Considering collapsars as sources for both HE neutrinos and r-process nuclei, we have investigated a novel effect on HE neutrinos caused by their annihilation with LE antineutrinos from the β decay of r-process nuclei. Assuming typical jet parameters, we have also discussed production of HE neutrinos at internal subshocks induced by mildly magnetized jets deep inside collapsars. Bright GRBs, LLGRBs, and choked GRBs may have a common origin in collapsars, and contributions to the diffuse HE neutrino flux are expected to be dominated by the latter two. Our collapsar model suggests that these sources can well account for the observed flux at IceCube, especially when annihilation with LE antineutrinos from β decay of r-process nuclei is included. Specifically, an excess at 10–100 TeV and potentially, a deficit at 0.1–1 PeV can be explained consistently for the IceCube events without overproducing the diffuse γ-ray background (see e.g., [106–109]).

A critical test of our HE neutrino production model is detection of precursor HE neutrinos (with a lead time of ~ 10–10^3 s) from nearby LLGRBs or bright GRBs. For an LLGRB at 100 Mpc with canonical parameters, IceCube-Gen2 can detect ~ 10 cascade events within 10–100 s if the jets are mildly magnetized. This short emission would also favor the speculation that LLGRBs host very similar jets to those in bright GRBs. Our model predicts a flavor composition at Earth close to that in the so-called muon-damped scenario at 10 TeV to 1 PeV, which can be distinguished from those in the standard pion and neutron decay scenarios [110–112] by precise measurements. The expected spectrum decays as $E^{-\gamma}$ at energies below ~ 100 TeV with $\gamma \sim 0.5$–1, followed by a steepening above 100–200 TeV due to the annihilation effect. Anticipating 10 years of data at IceCube-Gen2, we find that a spectral steepening with $\Delta\gamma > 1$ for our scenario can be observed at 95% CL (see the Supplemental Material [56]). In contrast, no clear break is expected without annihilation. The above neutrino signatures together with the r-process imprints in collapsar light curves can provide important support of collapsars as sources for both HE neutrinos and r-process nuclei.

We have made several simplifications in this initial study. Future improvements include detailed modeling of LE antineutrino emission, spatial and temporal variations of r-process production in collapsars, and self-consistent collapsar simulations for HE neutrino production. Finally,

the same annihilation effect should occur in BNSMs that host short GRBs and the r process, and can in principle be tested with a future nearby event.

[1] S. E. Woosley, Astrophys. J. **405**, 273 (1993).
[2] A. I. MacFadyen and S. E. Woosley, Astrophys. J. **524**, 262 (1999).
[3] S. E. Woosley and J. S. Bloom, Annu. Rev. Astron. Astrophys. **44**, 507 (2006).
[4] S. Campana et al., Nature (London) **442**, 1008 (2006).
[5] J. Hjorth and J. S. Bloom, in Chapter 9 in *Gamma-Ray Bursts* (Cambridge University Press, Cambridge, England, 2012), pp. 169–190.
[6] P. Kumar and B. Zhang, Phys. Rep. **561**, 1 (2014).
[7] P. Mészáros and E. Waxman, Phys. Rev. Lett. **87**, 171102 (2001).
[8] S. Razzaque, P. Meszaros, and E. Waxman, Phys. Rev. D **68**, 083001 (2003).
[9] S. Razzaque, P. Mészáros, and E. Waxman, Phys. Rev. Lett. **93**, 181101 (2004).
[10] S. Ando and J. F. Beacom, Phys. Rev. Lett. **95**, 061103 (2005).
[11] S. Razzaque, P. Meszaros, and E. Waxman, Mod. Phys. Lett. A **20**, 2351 (2005).
[12] S. Horiuchi and S. Ando, Phys. Rev. D **77**, 063007 (2008).
[13] R. Enberg, M. H. Reno, and I. Sarcevic, Phys. Rev. D **79**, 053006 (2009).
[14] I. Bartos, B. Dasgupta, and S. Marka, Phys. Rev. D **86**, 083007 (2012).
[15] K. Murase and K. Ioka, Phys. Rev. Lett. **111**, 121102 (2013).
[16] N. Fraija, Mon. Not. R. Astron. Soc. **437**, 2187 (2014).
[17] D. Xiao and Z. G. Dai, Astrophys. J. **790**, 59 (2014).
[18] A. Bhattacharya, R. Enberg, M. H. Reno, and I. Sarcevic, J. Cosmol. Astropart. Phys. 06 (**2015**) 034.
[19] K. Varela, S. Sahu, A. F. O. Oliveros, and J. C. Sanabria, Eur. Phys. J. C **75**, 289 (2015).
[20] I. Tamborra and S. Ando, Phys. Rev. D **93**, 053010 (2016).
[21] N. Senno, K. Murase, and P. Meszaros, Phys. Rev. D **93**, 083003 (2016).
[22] N. Senno, K. Murase, and P. Mészáros, J. Cosmol. Astropart. Phys. 01 (2018) 025.
[23] P. B. Denton and I. Tamborra, Astrophys. J. **855**, 37 (2018).
[24] P. B. Denton and I. Tamborra, J. Cosmol. Astropart. Phys. 04 (2018) 058.
[25] H.-N. He, A. Kusenko, S. Nagataki, Y.-Z. Fan, and D.-M. Wei, Astrophys. J. **856**, 119 (2018).

[26] P.-W. Chang, B. Zhou, K. Murase, and M. Kamionkowski, arXiv:2210.03088.
[27] E. Guarini, I. Tamborra, and O. Gottlieb, Phys. Rev. D **107**, 023001 (2022).
[28] M. G. Aartsen et al., Science **361**, eaat1378 (2018).
[29] M. G. Aartsen et al., Science **361**, 147 (2018).
[30] R. Stein et al., Nat. Astron. **5**, 510 (2021).
[31] S. Reusch et al., Phys. Rev. Lett. **128**, 221101 (2022).
[32] S. van Velzen et al., arXiv:2111.09391.
[33] R. Abbasi et al., Science **378**, 538 (2022).
[34] B. P. Abbott et al., Phys. Rev. Lett. **119**, 161101 (2017).
[35] B. P. Abbott et al., Astrophys. J. Lett. **848**, L12 (2017).
[36] D. Kasen, B. Metzger, J. Barnes, E. Quataert, and E. Ramirez-Ruiz, Nature (London) **551**, 80 (2017).
[37] M. R. Drout et al., Science **358**, 1570 (2017).
[38] P. S. Cowperthwaite et al., Astrophys. J. Lett. **848**, L17 (2017).
[39] V. A. Villar et al., Astrophys. J. Lett. **851**, L21 (2017).
[40] M. Shibata, S. Fujibayashi, K. Hotokezaka, K. Kiuchi, K. Kyutoku, Y. Sekiguchi, and M. Tanaka, Phys. Rev. D **96**, 123012 (2017).
[41] B. D. Metzger, Living Rev. Relativity **23**, 1 (2020).
[42] D. Watson et al., Nature (London) **574**, 497 (2019).
[43] D. M. Siegel, J. Barnes, and B. D. Metzger, Nature (London) **569**, 241 (2019).
[44] D. M. Siegel, Eur. Phys. J. A **55**, 203 (2019).
[45] P. Macias and E. Ramirez-Ruiz, Astrophys. J. Lett. **877**, L24 (2019).
[46] I. Bartos and S. Marka, Astrophys. J. Lett. **881**, L4 (2019).
[47] J. M. Miller, T. M. Sprouse, C. L. Fryer, B. R. Ryan, J. C. Dolence, M. R. Mumpower, and R. Surman, Astrophys. J. **902**, 66 (2020).
[48] S. Fujibayashi, M. Shibata, S. Wanajo, K. Kiuchi, K. Kyutoku, and Y. Sekiguchi, Phys. Rev. D **102**, 123014 (2020).
[49] K. Brauer, A. P. Ji, M. R. Drout, and A. Frebel, Astrophys. J. **915**, 81 (2021).
[50] J. Fraser and R. Schönrich, Mon. Not. R. Astron. Soc. **509**, 6008 (2022).
[51] J. Barnes and B. D. Metzger, Astrophys. J. **939**, L29 (2022).
[52] O. Just, M. A. Aloy, M. Obergaulinger, and S. Nagataki, Astrophys. J. Lett. **934**, L30 (2022).

[53] S. Fujibayashi, Y. Sekiguchi, M. Shibata, and S. Wanajo, arXiv:2212.03958.

[54] S. Anand *et al.*, arXiv:2302.09226.

[55] B. D. Metzger, G. Martínez-Pinedo, S. Darbha, E. Quataert, A. Arcones, D. Kasen, R. Thomas, P. Nugent, I. V. Panov, and N. T. Zinner, Mon. Not. R. Astron. Soc. **406**, 2650 (2010).

[56] See the Supplemental Material at http://link.aps.org/supplemental/10.1103/PhysRevD.108.L021303 for effects of the disk wind geometry and the LE antineutrino oscillation scenarios on annihilation between HE and LE neutrinos, timescales for acceleration and cooling of proton and charged mesons, and a sensitivity study on detecting a spectral steepening of the diffuse flux with IceCube-Gen2.

[57] S. Rosswog, O. Korobkin, A. Arcones, F. K. Thielemann, and T. Piran, Mon. Not. R. Astron. Soc. **439**, 744 (2014).

[58] M.-R. Wu, J. Barnes, G. Martinez-Pinedo, and B. D. Metzger, Phys. Rev. Lett. **122**, 062701 (2019).

[59] T. Hayakawa and K. Maeda, Astrophys. J. **854**, 43 (2018).

[60] W. Waxman and J. Bahcall, Phys. Rev. Lett. **78**, 2292 (1997).

[61] E. Waxman and J. N. Bahcall, Astrophys. J. **541**, 707 (2000).

[62] Z. Li, Z. G. Dai, and T. Lu, Astron. Astrophys. **396**, 303 (2002).

[63] D. Guetta, D. Hooper, J. Alvarez-Muniz, F. Halzen, and E. Reuveni, Astropart. Phys. **20**, 429 (2004).

[64] K. Murase and S. Nagataki, Phys. Rev. Lett. **97**, 051101 (2006).

[65] K. Murase, K. Ioka, S. Nagataki, and T. Nakamura, Astrophys. J. Lett. **651**, L5 (2006).

[66] K. Murase, Phys. Rev. D **76**, 123001 (2007).

[67] S. Hummer, P. Baerwald, and W. Winter, Phys. Rev. Lett. **108**, 231101 (2012).

[68] B. Zhang and P. Kumar, Phys. Rev. Lett. **110**, 121101 (2013).

[69] R.-Y. Liu and X.-Y. Wang, Astrophys. J. **766**, 73 (2013).

[70] M. Bustamante, P. Baerwald, K. Murase, and W. Winter, Nat. Commun. **6**, 6783 (2015).

[71] G. Nir, D. Guetta, H. Landsman, and E. Behar, Astrophys. J. **817**, 142 (2016).

[72] D. Biehl, D. Boncioli, A. Fedynitch, and W. Winter, Astron. Astrophys. **611**, A101 (2018).

[73] G. Guo, Y.-Z. Qian, and M.-R. Wu, Astrophys. J. **890**, 83 (2020).

[74] S. S. Kimura, arXiv:2202.06480.

[75] A. Levinson and O. Bromberg, Phys. Rev. Lett. **100**, 131101 (2008).

[76] B. Katz, R. Budnik, and E. Waxman, Astrophys. J. **716**, 781 (2010).

[77] A. M. Beloborodov, Astrophys. J. **838**, 125 (2017).

[78] C. Lundman and A. Beloborodov, Astrophys. J. **879**, 83 (2019).

[79] P. Crumley, D. Caprioli, S. Markoff, and A. Spitkovsky, Mon. Not. R. Astron. Soc. **485**, 5105 (2019).

[80] O. Gottlieb and N. Globus, Astrophys. J. Lett. **915**, L4 (2021).

[81] O. Gottlieb, O. Bromberg, C. B. Singh, and E. Nakar, Mon. Not. R. Astron. Soc. **498**, 3320 (2020).

[82] O. Gottlieb, O. Bromberg, A. Levinson, and E. Nakar, Mon. Not. R. Astron. Soc. **504**, 3947 (2021).

[83] T. Piran, Rev. Mod. Phys. **76**, 1143 (2004).

[84] P. Meszaros, Rep. Prog. Phys. **69**, 2259 (2006).

[85] P. Kumar and B. Zhang, Phys. Rep. **561**, 1 (2014).

[86] A. Mizuta and M. A. Aloy, Astrophys. J. **699**, 1261 (2009).

[87] A. R. Bell, Mon. Not. R. Astron. Soc. **182**, 147 (1978).

[88] C. Bierlich *et al.*, arXiv:2203.11601.

[89] A. Mucke, R. Engel, J. P. Rachen, R. J. Protheroe, and T. Stanev, Comput. Phys. Commun. **124**, 290 (2000).

[90] S.-X. Yi, W.-H. Lei, B. Zhang, Z.-G. Dai, X.-F. Wu, and E.-W. Liang, J. High Energy Astrophys. **13–14**, 1 (2017).

[91] R. Abbasi *et al.*, Nature (London) **484**, 351 (2012).

[92] M. G. Aartsen *et al.*, Astrophys. J. Lett. **805**, L5 (2015).

[93] M. G. Aartsen *et al.*, Astrophys. J. **824**, 115 (2016).

[94] M. G. Aartsen *et al.*, Astrophys. J. **843**, 112 (2017).

[95] R. Abbasi *et al.*, Astrophys. J. **939**, 116 (2022).

[96] A. M. Soderberg *et al.*, Nature (London) **442**, 1014 (2006).

[97] E. Liang, B. Zhang, and Z. G. Dai, Astrophys. J. **662**, 1111 (2007).

[98] E. Nakar, Astrophys. J. **807**, 172 (2015).

[99] E. Sobacchi, J. Granot, O. Bromberg, and M. C. Sormani, Mon. Not. R. Astron. Soc. **472**, 616 (2017).

[100] E. Waxman and J. N. Bahcall, Phys. Rev. D **59**, 023002 (1999).

[101] M. G. Aartsen *et al.*, Phys. Rev. Lett. **125**, 121104 (2020).

[102] C.-Y. Chen, P. S. Bhupal Dev, and A. Soni, Phys. Rev. D **92**, 073001 (2015).

[103] A. Palladino, C. Mascaretti, and F. Vissani, Eur. Phys. J. C **77**, 684 (2017).

[104] M. Chianese, R. Mele, G. Miele, P. Migliozzi, and S. Morisi, Astrophys. J. **851**, 36 (2017).

[105] K. Riabtsev and S. Troitsky, Phys. Lett. B **839**, 137758 (2023).

[106] K. Murase, D. Guetta, and M. Ahlers, Phys. Rev. Lett. **116**, 071101 (2016).

[107] K. Murase, S. S. Kimura, and P. Meszaros, Phys. Rev. Lett. **125**, 011101 (2020).

[108] A. Capanema, A. Esmaili, and K. Murase, Phys. Rev. D **101**, 103012 (2020).

[109] K. Fang, J. S. Gallagher, and F. Halzen, Astrophys. J. **933**, 190 (2022).

[110] M. G. Aartsen *et al.*, arXiv:1710.01207.

[111] M. G. Aartsen *et al.*, J. Phys. G **48**, 060501 (2021).

[112] N. Song, S. W. Li, C. A. Argüelles, M. Bustamante, and A. C. Vincent, J. Cosmol. Astropart. Phys. 04 (2021) 054.